Int. J. Electrochem. Sci., 13 **(2018)** 951 – 974, doi: 10.20964/2018.01.43

International Journal of
ELECTROCHEMICAL
SCIENCE
www.electrochemsci.org

Electrochemical, Thermodynamic and Quantum Chemical Studies of Synthesized Benzimidazole Derivative as an Eco-Friendly Corrosion Inhibitor for XC52 Steel in Hydrochloric Acid

Linda Toukal, Saida Keraghel[*]*, Fatiha Benghanem, Ali Ourari*

Laboratoire d'Electrochimie, d'Ingénierie Moléculaire et Catalyse Redox (LEIMCR)
Département de Génie des Procédés, Faculté de Technologie, Université Ferhat Abbas Sétif-1
E-mail : s_marouani20012002@yahoo.fr

Received: 20 June 2017 / *Accepted:* 12 October 2017 / *Online Published:* 16 December 2017

This work focuses on the study of the inhibitory action of an heterocyclic compound, 1-(4-methoxybenzyl)-2-(4-methoxyphenyl)-1H-benzimidazole (MMBI) against corrosion of a steel pipeline sample grade XC52 in a 1M hydrochloric acid (HCl) solution. The electrochemical methods as the impedance spectroscopy and the potentiodynamic polarization were used to perform this investigation. The effect of the MMBI concentration and the temperature was studied. The determined electrochemical parameters showed that MMBI is a good inhibitor against the corrosion of XC52 steel in 1M HCl at a concentrations range from 510^{-6} to 10^{-4}M of benzimidazole and temperature ranging from 20 to 60 °C. The inhibiting efficiency (EI%) and the apparent activation energy (E_a) have been calculated in the absence and in the presence of MMBI. The inhibition rate increased with the MMBI concentration to reach 93% for 10^{-4}M as optimum inhibitor concentration. Potentiodynamic polarizations showed the effect of presence of MMBI on the anodic and cathodic processes suggesting that MMBI can be a mixed type inhibitor. The mechanism of the action of this inhibitor was defined by the thermodynamic study. The calculated values of $\Delta G°_{ads}$, ΔH_a, E_a and ΔS_a showed that the 1-(4-methoxybenzyl)-2-(4-methoxyphenyl)-1H-benzimidazole strongly retards the corrosion of the XC52 steel in 1M HCl solution according a chemisorption process. The adsorption phenomenon of this compound on the carbon steel obeys to a Langmuir adsorption isotherm. The quantum chemical parameters were calculated by the Density Functional Theory method (DFT). The experimental and theoretical results are coherent and agree with those of the literature.

Keywords: Corrosion inhibitor, Steel XC52, 2-Aryl-1-arylmethyl-1H-benzimidazole, Potentiodynamic polarization, Impedance spectroscopy, DFT-Calculations.

1. INTRODUCTION

In the petroleum industry, statistical reported data indicate that important losses are caused by corrosion failures of pipelines [1]. Corrosion is not only a source of wastage of raw materials; it can also lead to major economic and human losses with irremediable ecological tragedies. The corrosive HCl solution is widely used for petroleum industry. The instability of steel in corrosive media such as HCl solution causes oxidation of this metal. XC52 steel widely used for pipelines is subject to corrosion in 1M HCl. As of the strong corrosivity of the acid solution, the use of corrosion inhibitors, added in the liquid phase, constitutes the best mean for corrosion protection in many industrial systems particularly the oil industry because it offers considerable savings. Organic inhibitors were used in petroleum refining processes given that they can form a protective layer on the metal surface. These inhibitors were adsorbed on the metal surface with the coordinate covalent bond (chemical adsorption) or electrostatic interactions (physical adsorption) [2].

The action of an organic corrosion inhibitor depends on the type of the environment in which it acts [3-5]. In the literature, there is a number of organic inhibitors such as fatty amides [6, 7], pyridines [8-10], imidazolines [11, 12], 1,3-azoles [13-15] and polymers [16] which have a good performances. Matjaž Finšgar and al. [17] have reported some corrosion inhibitors for steels in acidic media. This review presented works on the steel corrosion inhibition in the industrial fields. Among them, heterocyclic compounds containing O, N, S heteroatoms and aromatic entities with their sp^2 and sp hybridization systems from with useful interactions were developed. The corrosion inhibiting properties of this type of compounds are due to the ability of the heteroatoms to give electrons, to the co-planarity of the heterocyclics (p-bonds) with its electronic delocalization facilitating the adsorption of these molecules on the metallic surface [18-20]. The benzimidazole and its derivatives constitute good inhibitors for mild steel [21]. In recent years, these organic molecules have received attention due to their inhibition effects towards metallic corrosion. It has been shown that they are effective inhibitors for metals in acidic solutions. The adsorption is more facilitated by the presence of the aromatic rings and the heteroatom such nitrogen [22-28].

Popova *et al*. [29] have studied benzimidazole, 2-mercaptobenzimidazole, 2-aminobenzimidazole, 1,2-dibenzylbenzimidazole, and 1-benzylbenzimidazole as corrosion inhibitors for mild steel in 1M HCl solution. These diazoles have presented corrosion inhibition characteristics and three of these latter revealed a particular effectiveness. The same authors [30], investigated other mixed type inhibitors benzimidazole derivatives. They concluded that the rate of inhibition of these compounds was in a decreasing order according the following sequence: 2-mercaptobenzimidazole >.2-benzimidazolylacetonitrile > 2-aminobenzimidazole > 2-hydroxymethylbenzimidazole > 5(6)-carboxybenzimidazole > 2-methylbenzimidazole > benzimidazole > 5(6)-nitrobenzimidazole.

In order to explain their results, Popova *et al*. [31] have investigated other compounds. They reported that benzimidazole has the lowest inhibition rate. They concluded that these investigated compounds are mixed-type inhibitors, and that they reduce predominantly the rate of the anodic reaction. Aljourani *et al*. [32] have as well confirmed that benzimidazole exhibits the lowest inhibition rate. It has to be noted that the values of EI(%) calculated from the experimental results are different at the highest inhibitor concentration. On the other hand Abboud *et al*. [24] have investigated the

efficiency of 2-(o-Hydroxyphenyl)benzimidazole against the acidic corrosion of steel. The obtained results revealed that this compound has an efficiency of around 93% at a concentration of 500μM. This inhibitor was found to be belonging to a mixed type with predominance of the anodic character as it was mentioned above [31]. Xiumei et al. [22] who have studied the Bis-benzimidazole molecule reported that experiment data showed an excellent inhibition effect against steel corrosion in hydrochloric acid due to the planarity of the benzimidazole ring, which show a big projected area on the metal surface of this kind of molecules. The importance of the mechanism of corrosion inhibition and its relation with electronic and structural properties of the inhibitor molecules has attracted attention to quantum chemical calculation. This method has been used to study quantitatively the relationship between inhibition efficiency and molecular reactivity, and can also be used to evaluate the effectiveness of corrosion inhibitors [33-35].

The Density Functional Theory (DFT) calculations were performed to explore the electronic properties associated to molecular structure and the adsorption ability of benzimidazole derivatives onto carbon steel [33, 36-39]. So, it was demonstrated that the efficiency of organic inhibitors is affected by their structure. The corrosion inhibition of organic compounds increases when the HOMO energy level increases [40] and the HOMO-LUMO energy gap value decreases. Some authors [41-43] noted that the inhibitory power is affected by the polarity of the organic compound.

It was showed [44-46] that the heteroatoms play an notably role in the inhibiting mechanism. The presence of nitrogen atom and the aromatic rings of the benzimidazole molecule facilitate the adsorption of compounds on the metallic surface [11,47].

To our knowledge, and according to the literature quoted above, it can be noted that benzimidazole and its derivatives with aromatic substituents (2-aryl-1-arylmethyl-1H-benzimidazoles) have not been studied as corrosion inhibitors in an acidic medium against XC52 steel. In this context and as a continuation of previous research on acid corrosion inhibitors of XC52 steel, we report herein the investigation on the corrosion inhibition performances of the eco-friendly inhibitor: 1-(4-methoxybenzyl)-2-(4-methoxyphenyl)-1H-benzimidazole (MMBI) against corrosion of a pipeline steel sample grade XC52 in 1M hydrochloric acid solution. Electrochemical potentiodynamic polarization, impedance spectroscopy method, and quantum chemical calculations were used to realize this work. The Density Functional Theory calculation was used to investigate the interaction mechanism between the neutral molecule and the steel surface in a corrosive medium in gas and aqueous phase.

2. EXPERIMENTAL

2.1. Synthesis of 1-(4-Methoxybenzyl)-2-(4-methoxyphenyl)-1H-benzimidazole (MMBI)

The preparation of 1-(4-Methoxybenzyl)-2-(4-methoxyphenyl)-1H-benzimidazole (MMBI) (Scheme 1) investigated in this work was carried out according to the literature [48]. No catalyst substance was used in this selective and eco-friendly procedure for the synthesis of this substituted benzimidazole. To an amount of 4-methoxybenzaldehyde (1ml, 5.5mmol), dissolved in MeOH (10ml), was slowly added a solution of 1, 2-diaminoaniline (0.3g, 2.77mmol) in MeOH (10ml). The obtained

mixture was refluxed, and stirred under dinitrogen atmosphere for 24 hours. The precipitate was filtered and washed several times with cold methanol and finally with diethyl ether. The results of 1H-NMR and 13C-NMR, elemental analysis and mass spectrometry confirm the structure of the expected product

m.p. 130 °C; Chemical shifts in ppm: δHC-N(2H, s = 5.46); δHarom.((12H, m = 7.75–6.85; δCH_3O (6H, 2s = 3.75, 3.87). 13C NMR (400 MHz MeOD): δ-Chemical shifts in ppm: 48.39,48.60,48.81,49.02,49.24,49.45,55.73,55.96,112.15,115.4,119.62,123.09,124.19,128.58,129.88,131.93,137.00,143.43,155.51,160.78,162.87.Microanalysis of C22H20N2O2: Calc. (%): C 76.72; H 5.85; N 8.13 %Found (%): C 77.12, H 5.80, N 8.04%.ESI-MS [M^+ + $1H^+$] m/z 345.16067; ^{1}H-, NMR and ^{13}C-NMR spectra were measured on a Bruker AVANCE 400 MHz spectrometer using tetramethylsilane (TMS, d =0 ppm) as an internal standard. Mass spectra (MALDI-TOF-MS) were determined on a Bruker BIFLEXIII mass spectrometer. The spectroscopic parameters found are in agreement with those of the literature [49-52]. The molecular structure of MMBI is presented in the following scheme 1:

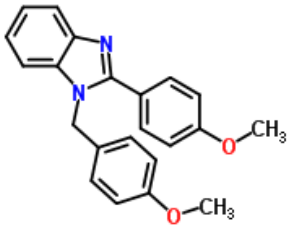

Scheme 1. Molecular structure of 1-(4-Methoxybenzyl)-2-(4-methoxyphenyl)-1H-benzimidazole.

2.2. Metal specimen

The working electrode was a mild steel XC52 grade with the following chemical composition (wt. %): 0.1038% C, 0.1261% Si, 0.0320% Al, 0.0021% S, 0.971% Mn, 0.0100% Cu, 0.1261 Si, 0.0021 P, 0.0100 Cr, 0.005 Mo, 0.0050 Ni, 0.0500 Co, 0.0100 Cu, 0.0419 Nb, 0.0025 V, 0.0500 W, 0.0050 Sn and 98.7% Fe. The surface of the steel specimen was polished with SiC paper of 380–2500 grit, degreased with acetone and rinsed with double distilled water, before immersion in the acid solution.

2.3. Solution

The corrosive medium is a solution of 1M hydrochloric acid, prepared from HCl 37% and double distilled water. The concentration of the inhibitor was in the range of 5.10^{-6}–10^{-4}M.

2.4. Electrochemical investigations

The electrochemical impedance measurements (EIS) and the potentiodynamic polarization curves were recorded using a PGZ 301 Potentiostat Galvanostat, VOLTALAB 40 type radiometer mark, driven by a "Voltamaster4" software and connected to a computer. Experiments were carried out in a thermostatted cell. A platinum plate was employed as the counter electrode (CE) and a silver–silver chloride (Ag/AgCl/KCl) electrode was used as the reference electrode (RE). The working electrode (WE) was a mild steel XC52 grade. All tests were performed at room temperature. Before recording the polarization curves, the freshly polished electrode was immersed in the working solution at open circuit potential for 30 minutes until a steady state was reached. The impedance spectroscopy measurements were carried out in the frequency range 10^5 – 10Hz at the open circuit potential with superimposing a sinusoidal AC signal of small amplitude, 10mV peak to peak. The intensity-potential curves are plotted in the potentiodynamic mode. After recording the cathodic branch, the open-circuit potential was then reestablished before determining the anodic branch. The potential applied to the sample was varied from -600 to -200mV vs. Ag /AgCl/KCl with a sweep rate equal to $2mV.s^{-1}$ which enables to perform tests under quasi-stationary conditions.

The corrosion inhibition efficiency EI(%) was determined from corrosion currents calculated from Tafel extrapolation method using the following relationship:

$$EI(\%) = \frac{I_{corr} - I_{corr(inh)}}{I_{corr}} \times 100 \qquad (1)$$

where I_{corr} and $I_{corr(inh)}$ are the corrosion current density values without and with the inhibitor, respectively, determined by extrapolation of the cathodic and anodic Tafel lines to the corrosion potential.

The values of R_t and C_{dl} were obtained from Nyquist plots. All measurements were carried out at the open circuit potential (E_{ocp}).

2.5. Theoretical calculations

Theoretical calculations were carried out using the DFT method (at B3LYP) functional with 6-31 G (d,p) basis set for all atoms in the gas and aqueous phases [53,54]. Using the standard Gaussian 09W software package [55, 56], the geometry of the synthesized molecular structure was optimized. The quantum chemical parameters were determined. The absolute electronegativity (χ), electrophilicity index (ω), dipole moment (μ), global hardness (η) and softness (σ), electron affinity (A), ionization potential (I), energy gap (ΔE), and the number of transferred electron (ΔN) for the benzimidazole MMBI were calculated using the following equations:

$$\chi = I + A/2 \qquad (2)$$

$$\eta = I - A/2 \qquad (3)$$

where, according to Koopmans' theory [57], I and A are related to the frontier orbital energies according to equations (4) and (5):

$$I = -E_{HOMO} \quad (4)$$

$$A = -E_{LUMO} \quad (5)$$

The values of χ and η for the benzimidazole studied were calculated using the values of I and A obtained from the quantum chemical calculations.

The number of transferred electrons (ΔN) was calculated using the following equation:

$$\Delta N = (\chi_{Fe} - \chi_{Inh})/2\,(\eta_{Fe} + \eta_{Inh}) \quad (6)$$

where χ_{Fe} and χ_{Inh} are the absolute electronegativities of iron and inhibitor, and η_{Fe} and η_{Inh} are the absolute hardnesses of iron and the inhibitor respectively. The theoretical χ value of 7.0eV mol^{-1} and η value of zero eV mol^{-1} for iron were used from the literature [58, 59].

The softness (σ) and the electrophilicity index (ω) were obtained using the following equations:

$$\sigma = 1/\eta \quad (7)$$

$$\omega = \chi^2/2\eta \quad (8)$$

3. RESULTS AND DISCUSSION

3.1. Potentiodynamic polarization measurments

The polarization curves for the investigated XC52 steel in 1M HCl solution in the presence and absence of MMBI at various concentrations are shown in Fig. 1. The corrosion potential (E_{corr}), corrosion current density values (I_{corr}), the cathodic and anodic Tafel slopes (b_c and b_a), and the inhibition efficiency EI (%) for different concentrations of MMBI in HCl are summarized in Table 1. As illustrated, all reactions of mild steel electrode corrosion were affected after addition of MMBI to the acidic medium but the cathode is more polarized ($b_c > b_a$). According to the shape of the obtained Tafel lines, it can be observed that the addition of MMBI is systematically translated by a decrease in the current densities. This shows that MMBI is adsorbed on the metal surface and the inhibition process occurs. The higher concentration of the MMBI leads to an elevated inhibition efficiency causesed by a higher coverage of inhibitor on the surface. The increasing of the anodic and cathodic Tafel slope indicates that the presence of the inhibitor retards the steel dissolution and also reduces the rate of the hydrogen ions reduction. The Tafel slopes variations suggest that MMBI influences the kinetics of the hydrogen reduction and metal ions formation [60]. This implies that the studied compound was first adsorbed onto the metal surface involving the blocking of the sites on the metal surface without acting on the anodic reaction mechanism [61].

This result can be explained by the barrier effect [62]. Bockris and Srinivasan explained that such behavior reflects the decrease of the cathodic transfer coefficient and therefore can be attributed to the thickening of the electric double layer due to the adsorbed inhibitor molecules [63].

According to table 1, there is no regular variation of E_{corr} as a function of the concentration of the inhibitor. The compound acts as a mixed inhibitor by reducing the rate of cathodic and anodic reaction. The respective reaction sites on the metal surface were blocked.

The addition of the inhibitor does not modify the mechanism of evolution and the reduction of hydrogen on the metal surface. The process follows a charge transfer mechanism [64]. This is demonstrated by the parallel Tafel lines (Fig.1). The inhibitor may be classified as cathodic or anodic type if the displacement in E_{corr} on addition of inhibitor is greater than 85mV with respect to the corrosion potential of the blank. While, when this displacement is less than the last value, the inhibitor may be considered as mixed-type [61]. The experimental results confirm that MMBI is a mixed type inhibitor with a predominant cathodic effectiveness. The inhibition efficiency determined (72%) at low concentration (5.10^{-6}M) reached 93% at a concentration of 10^{-4}M. These good inhibitive properties may be causes by the adsorption of MMBI molecules on the XC52 steel surface. The high molecular planarity of the heterocyclic compound (MMBI), the presence of electron donation groups and aromatic rings cause probably the performance of this inhibitor [22]. The nitrogen atom of C=N, the oxygen atom of O-CH_3 with their lonely sp^2 electron pair and the orbitals p of the aryl rings are suitable anchoring sites. This effect involves therefore the blocking of the active sites in the steel surface and decreasing the corrosion rate [62].

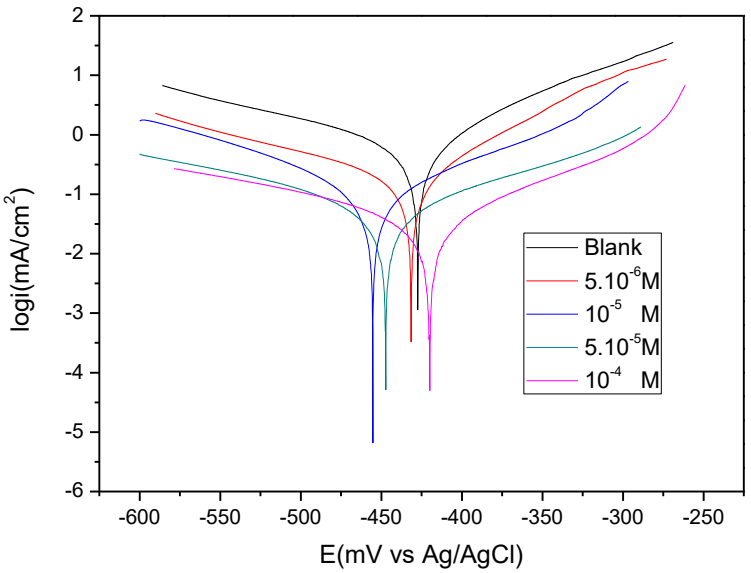

Figure 1. Tafel lines for the corrosion of XC52 steel in 1M HCl in the presence and absence of different concentrations of MMBI at 20°C.

Table 1. Electrochemical parameters of corrosion of XC52 steel in 1M HCl in the presence and absence of different concentrations of MMBI.

C (M)	i_{corr} (mA/cm^2)	$-E_{corr}$ (mV/ Ag/AgCl)	b_a ($mV.dec^{-1}$)	$-b_c$ ($mV.dec^{-1}$)	EI (%)
blanc	0.63	427	82	159	
5.10^{-6}	0.18	432	72	149	72
10^{-5}	0.14	455	117	126	77
5.10^{-5}	0.08	447	143	194	88
10^{-4}	0.04	420	109	200	93

3.2. Electrochemical impedance (EIS) measurements

The corrosion behavior of XC52 steel in 1M HCl in the presence and absence of aryl-benzimidazole (MMBI) inhibitor was investigated using the EIS method. The effect of inhibitor concentrations on the electrochemical behavior of XC52 steel in 1M HCl solution is seen in Fig.2. It can be observed that all the Nyquist plots obtained are semicircular and their diameters are affected by the evolution of the inhibitor concentration. The impedance response was significantly changed. The impedance of the XC52 steel electrode in HCl medium and in the presence of MMBI increases with elevating concentration of this inhibitor. This fact is due to the enhancement of the surface coverage of the inhibitor molecules on the electrode area [65]. This involves an increase in the inhibition rate. The semicircles obtained are depressed into the Z(real) of Nyquist plot, which is often due to a frequency dispersion resulting of the non homogeneity and/or roughness of the metal surface [66]. In order to establish a model for the mild steel/solution interface in the presence and absence of the inhibitor, the obtained EIS data were fitted to the electrical equivalent circuit shown in Fig. 3. The circuit consists of R_s, the electrolyte resistance, R_{ct}, the charge transfer resistance, and CPE the constant phase element [34]. The CPE replace the double layer capacitance (C_{dl}) in order to give a more accurate fit to the experimental results [64, 67]. CPE is recommended to be used for modeling the frequency dispersion generally related to the heterogeneity surface [68].

The Fig.4 shows the plots (Bode impedance magnitude and phase angle) recorded for XC52 steel electrode immersed in 1M HCl with and without different concentrations of MMBI. The Bode plots indicate the existence of an equivalent circuit containing a single constant phase element in the metal/solution interface. It is seen that the protection is better at high concentrations of the inhibitor. This is confirmed by the increase of the absolute impedance at low frequencies in the Bode plots [69]. The more negative values of the phase angle indicate that the good inhibitive behavior is caused by the more inhibitor molecules adsorbed on XC52 steel surface at higher concentrations. The observation of a single phase peak in the central frequency range shows the existence of a single constant, linked to the electric double layer [70]. The impedance characteristics, obtained from Nyquist plots, are given in Table 2. The resistance, R_p values are calculated from the difference in impedance at lower and higher frequencies [71, 72].

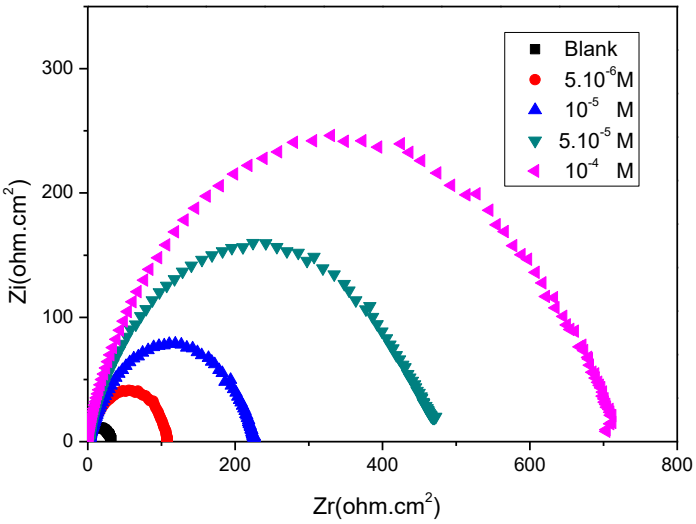

Figure 2. Nyquist plots for XC52 steel in 1M HCl in the presence and absence of different concentrations of MMBI at 20 °C.

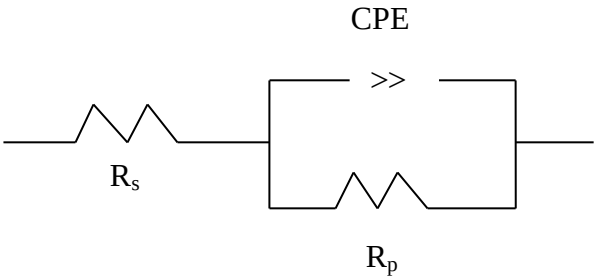

Figure 3. Electrochemical equivalent circuit used for simulation of the impedance spectra.

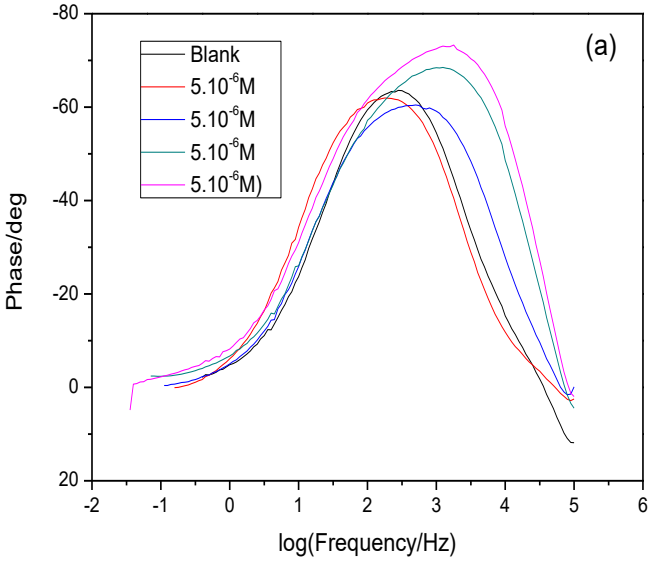

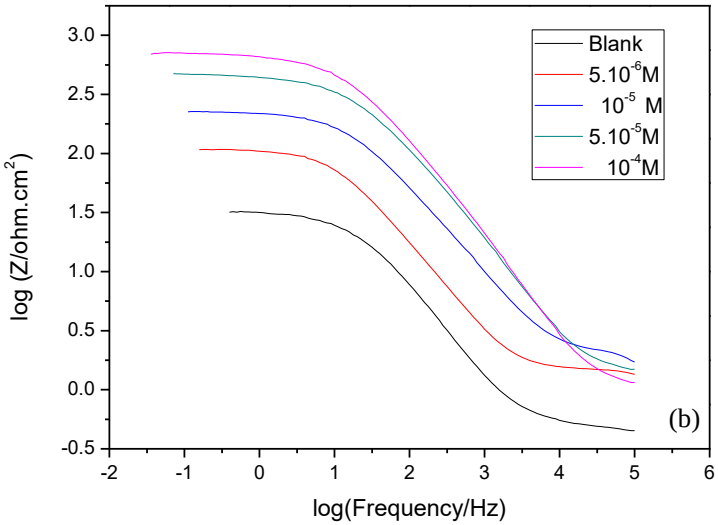

Figure 4. Bode (a) and phase angle (b) plots for XC52 steel in 1M HCl in the presence and absence of different concentrations of MMBI at 20 °C.

The double capacitance (C_{dl}) values are obtained from the following equation:

$$f(-Z_{max}) = \frac{1}{2\pi C_{dl} R_p} \quad (9)$$

The inhibition efficiency is calculated from the equation (10):

$$EI\ (\%) = \frac{R_{pinh} - R_p}{R_{pinh}} \times 100 \quad (10)$$

where R_p and R_{pinh} are the charge transfer resistance values without and with MMBI, respectively.

Table 2. Electrochemical impedance parameters for XC52 steel in 1M HCl in the presence and absence of different concentrations of MMBI at 20 °C.

C(M)	**R_s(mohm /cm^2)**	**R_P(ohm /cm^2)**	**C_{dl}(µF /cm^2)**	EI**(%)**
Blanc	368	32	249	-
5.10^{-6}	0.002	107	133	70
10^{-5}	0.002	224	40	86
5.10^{-5}	7.18	465	19	93
10^{-4}	0.59	679	17	95

Table 2 indicates that elevating the concentration of MMBI results the decrease of C_{dl} values and an increase of the inhibitor efficiency rate. This decrease in C_{dl} is explained by a decrease in the local dielectric constant and/or an increase in the thickness of the electric double layer, resulting from the adsorption of the MMBI molecules [73]. These results clearly indicate that the corrosion of XC52 steel in 1M HCl solution is controlled by a charge transfer process [74]. To summarize, obtained results from these electrochemical technique in 1M HCl solutions were coherent with those obtained from the potentiodynamic polarization method.

3.3. Adsorption isotherm

The adsorption isotherms can provide important information on the interaction between the organic compounds and the metal surface. In order to determine the free energy of adsorption and to demonstrate the adsorption characteristics of the MMBI on XC52 steel surface we have tested several types of adsorption isotherms. We found that Langmuir adsorption isotherm was the best suited for fitting of the obtained experimental results. The recovery rate θ given for various concentrations of the inhibitor in an acidic medium is evaluated from the polarization curves using the following equations:

$$\theta = I_{corr} - I_{corr(inh)} / I_{corr} \quad (11)$$

$$C_{inh}/\theta = 1/K_{ads} + C_{inh} \text{ (Langmuir isotherm)} \quad (12)$$

where θ is the fractional surface coverage; C_{inh} is the inhibitor concentration, and K_{ads} is the equilibrium constant of the adsorption phenomenon.

By plotting C_{inh}/θ versus C_{inh} (Fig.5), the value of K_{ads} was calculated.

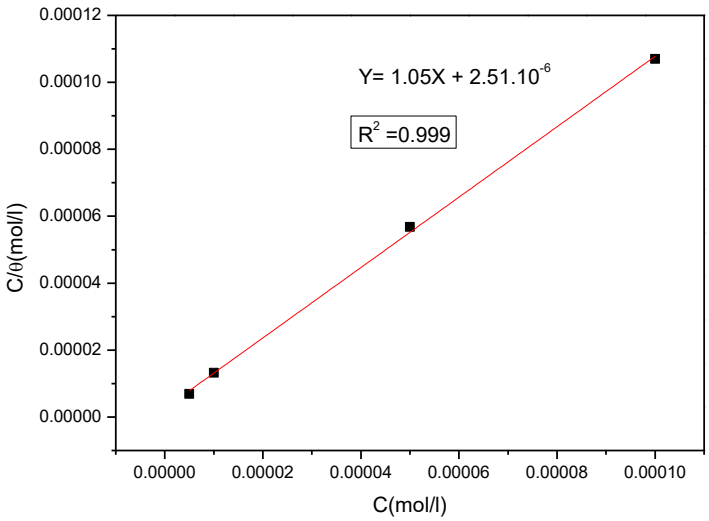

Figure 5. Langmuir presentation of MMBI inhibitor for XC52 steel in 1M HCl at 20 °C.

A linear fit is noted (R^2=0.999). The slope being close to unity indicates that the adsorption of MMBI on the steel surface in hydrochloric acid follows the Langmuir adsorption isotherm without interaction between the adsorbed species on the steel surface [75]. The equilibrium constant of the adsorption value (K_{ads}=3.98 10^5) was determined from the intercepts of the straight line C_{inh}/θ – axis. A good correlation of this value with the literature [3, 61] is observed (K_{ads} is of the order of $10^5 M^{-1}$). According to [76], the value of $\Delta G°_{ads}$ for the inhibitor is calculated from the equation (13):

$$\Delta G^0_{ads} = -RT \ln(55.55 K_{ads}) \quad (13)$$

where R is the universal gas constant, T the thermodynamic temperature and the value 55.55 in the above equation is the concentration of water in solution expressed in mol/l. Generally, if the value of $\Delta G°_{ads} \leq$-20KJ/mol this indicates to electrostatic interactions between the metal charge and the charged molecules (physisorption), but if $\Delta G°_{ads} \geq$ -40KJ/mol this involves a transfer of charges between the organic molecules and the metal surface (chemisorption) [77]. In this work the value of $\Delta G°_{ads}$ calculated is -41.87kJ/mol which shows that this inhibitor is chemisorbed on the metallic surface. These results are coherent with the literature [3, 5, 22, 77, 78]. The spontaneity of the adsorption process and the stability of the adsorbed double layer on the metal surface are confirmed by the negative value of $\Delta G°_{ads}$ [5].

3.4. Effect of temperature

The temperature can affect the metal-inhibitor interactions. To confirm the effect of this parameter on the inhibitory power of the studied organic compound, an investigation was carried out between 20 and 60°C. Tafel lines of XC52 steel in HCl 1M solution in absence and in presence of MMBI were plotted in this temperature range (Fig.6).

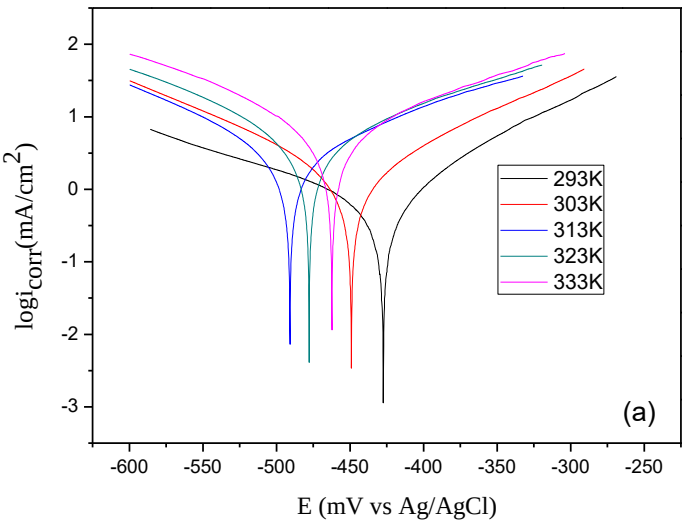

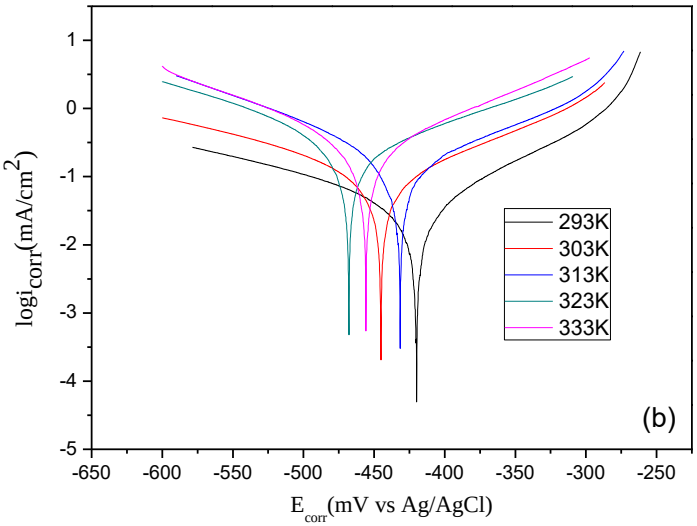

Figure 6. Tafel curves for the corrosion of XC52 steel in 1M HCl in the absence (a) and presence (b) of 10^{-4}M of MMBI at different temperatures.

Corrosion parameters and inhibition efficiency EI(%) for different temperatures are given in Table 3.

Table 3. Electrochemical characteristics of corrosion of XC52 steel in 1M HCl as a function of temperature.

	Temperature (K)	$I_{corr.}$ (mA/cm^2)	$-E_{corr}$(mV/Ag/AgCl)	b_a (mV.dec^{-1})	$-b_c$ (mV.dec^{-1})	EI (%)
HCl 1M	293	0.63	427	82	159	/
	303	1.76	449	114	121	/
	313	3.21	491	145	118	/
	323	6.13	478	173	140	/
	333	8.65	462	168	147	/
HCl 1M +MMBI 10^{-4} M	293	0.04	420	109	200	93
	303	0.13	445	142	207	93
	313	0.22	431	147	138	93
	323	0.37	468	170	189	94
	333	0.34	456	129	142	96

It is noted that the current densities and the inhibition efficiency increase with the temperature enhancement. The curves in the cathode part are parallel showing that the reduction of the H^+ at the steel surface takes place according to the same mechanism. It can also be noted that the cathodic Tafel slope slightly vary with temperature, while the anodic one increases. E_{corr} shifts in the negative direction. These results agree with the literature [27]. The MMBI has a remarkable inhibitor efficiency of about 96%. This structure is very effective because of the nitrogen atom of the heterocycle, the oxygen atom of O-CH_3 and the aryl rings. It is demonstrated that the elevation in the temperature produces an increase in the electron density around the adsorption sites [79]. Arrhenius equation (14) gives the dependence of the corrosion rate with temperature.

$$I_{corr} = k\exp\left(\frac{-Ea}{RT}\right) \quad (14)$$

where E_a represents the activation energy of discharge of the hydrogen ions, R is the gas constant, T the temperature and K the pre-exponential factor.

Thermodynamic characteristics of the corrosion reaction such as: Ea, ΔS_a and ΔH_a were obtained from Arrhenius Eq. (14) and its alternative formulation, named transition state equation (15):

$$I_{corr} = RT/N\ h \exp(\Delta S_a /R) \exp(-\Delta H_a /RT) \quad (15)$$

where h is Plank's constant and N is Avogadro's number. Fig. (7 and 8) show the Arrhenius plots in the absence and presence of MMBI for a temperature range of (293-333K). From the Fig.7 the values of Ea and the pre-exponential factor K are determined.

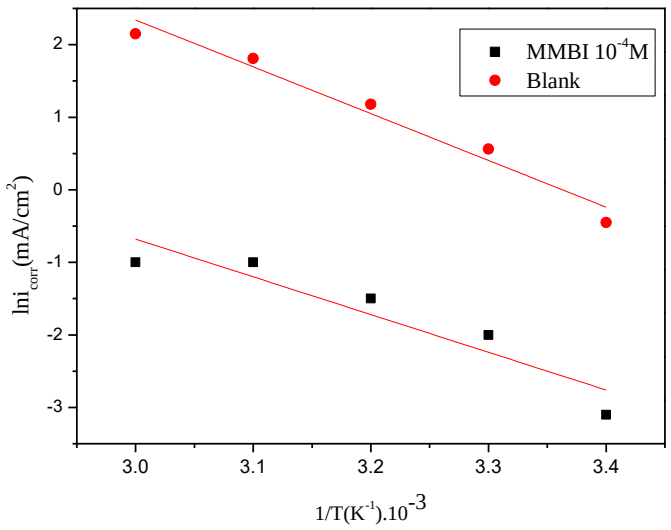

Figure 7. Arrhenius plots for the corrosion of XC52 steel in 1M HCl in the presence and absence and presence of 10^{-4}M of MMBI at different temperatures.

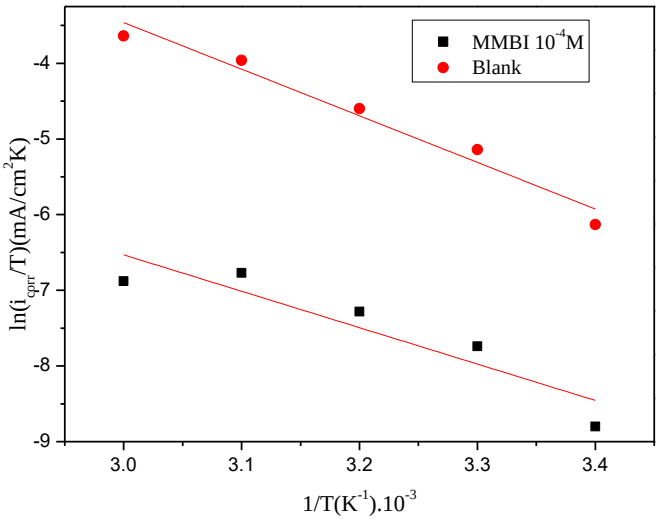

Figure 8. Transition state curves for the corrosion of XC52 steel in 1M HCl in the presence and absence of 10^{-4}M of MMBI at different temperatures.

The thermodynamic parameters obtained from equation (15) are summarized in Table 4.

Table 4. Activation characteristics for the adsorption of MMBI on XC52 steel surface.

	E_a(KJ/mol)	ΔH_a(KJ/mol)	ΔS_a(J/mol.K)
1M HCl	53.6	51.19	-72.23
1M HCl + MMBI 10^{-4}M	42.38	40.00	-131.38

The value of Ea in the presence of the inhibitor is smaller than its value in the pur acidic solution. This result is attributed to the chemisorption of MMBI on the surface of the steel [65, 80]. The value of the enthalpy (40KJ/mol) being positive confirms the endothermic dissolution of steel [81]. These results agree with the chemisorption mechanism [65]. The high and negative entropy value (ΔS_a=-131.38J/mol.K) indicates that the activated complex formed in the limiting step, exhibits an association rather than dissociation. This signifies that the disorder is reduced when the reactants are transformed into an activated complex. We note a good accordance of our results with the literature [82, 83]. When $E_{ainh}<E_{aHCl}$ the adsorbed species cover a larger number of sites. Therefore, the activation energy becomes lower because less adsorption sites are available for the corrosion process.

3.5. Quantum chemical study and mechanism of inhibition action

To study the effect of the electronic properties and molecular structure towards the inhibition effectiveness of the MMBI benzimidazole derivative and to confirm or infirm the experimental data obtained from electrochemical experiments, a quantum chemical calculation has been applied. The

optimized structure, the Mullikan charges density and the frontier molecular orbital density distributions (HOMO and LUMO) of MMBI given by the B3LYP/6-31G (d,p) method are shown in Fig.9.

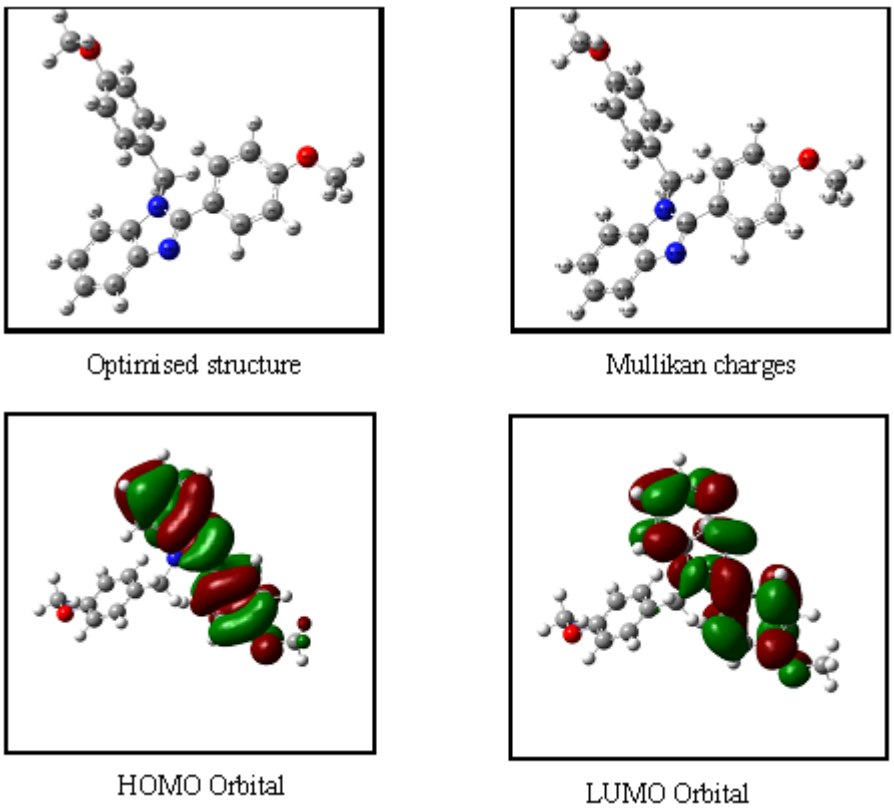

Figure 9. Optimized structure, Mullikan charges density and the frontier molecular orbital density distribution (HOMO and LUMO) of MMBI given by the B3LYP/6-31(d.p.)

The quantum chemical characteristics such as: E_{HOMO}, E_{LUMO}, ΔE_{L-H}, μ, χ, η, σ, ω and ΔN affect the inhibitor efficiency [84]. The equations from 1 through 7 have been used to evaluate these quantum chemical parameters for the estimated structure of the neutral MMBI in gas and aqueous phases (Table 5).

Table 5. The calculated quantum chemical parameters for the studied MMBI inhibitor in the gas and aqueous phase obtained using the DFT method at the B3LYP/6-31G(d,p) basis set.

Quantum parameters	Gas phase	Aqueous phase
E_{tot}(eV)	-30214.72	-30215
E_{Homo}(eV)	-5.44	-5.71
E_{Lumo}(eV)	-0,76	-1.00
ΔE_{GAP} (eV)	4.68	4.70
μ(Debye)	2,62	6.20
η(eV)	2.34	2.35

σ	0.43	0.43
χ(eV)	3.1	3.36
ω	2.05	2.40
ΔN	0.83	0.71

The HOMO and LUMO energies and ΔE agree with the inhibition efficiency [34, 77]. It is known that in most cases, the decrease of ΔE and E_{LUMO} as well as the increase of E_{HOMO} involves the increase of inhibitors efficiency. A high value of E_{HOMO} leads to a stronger chemisorption and higher inhibition behavior for the metal. Small E_{LUMO} values increase the possibility of the molecule to accept electrons. Moreover, the lower ΔE can cause stronger chemisorption of the inhibitor molecules on the metal area [85]. When ΔE value is low, the removing electrons from HOMO need a small energy. This confirms the experimental results obtained and is also in accordance with the values obtained from ΔN calculated using equation (6) [86, 87]. The values of the global hardness and the electronegativity for benzimidazole MMBI were obtained using the values of the frontier orbital energies calculated from the quantum chemical calculations. The examination of the presented data in Table 5, shows that the high value of E_{HOMO}= −5.44eV of the studied compound reveals the elevated inhibition efficiency [88]. It was demonstrated that an inhibitor can accept electrons from the d orbital of the metal or donate an electron to the unoccupied d orbital of the metal ion leading to the formation of a covalent bond. Therefore, the formation of this last depends on the value of E_{LUMO}. The low value of the E_{LUMO} = − 0.76eV shows the easiness of the receipt of electrons from the d orbital of the metal [89, 90]. The $\Delta E = E_{LUMO} - E_{HOMO}$ parameter affects the power of the adsorption of the inhibitor molecule on the metallic area. As ΔE decreases, the action of the inhibitor increases. The found results indicate that our inhibitor has a low value of energy gap (4.68eV) which confirms the experimental conclusions and the reactivity of the molecule with metal atoms.[33,34]. The inhibitive ability of a molecule is related to the dipole moment (μ) [65]. The elevated value of μ may increase the adsorption. Therefore, this phenomenon can be considered as a quasi-substitution process between the inhibitor molecule in the aqueous phase and water molecules on the XC52 steel area, with desorption of water molecules from the metal. Thus, the protection of the steel can be occurred. The value of μ_{inb} (2.62Debye) (Table 5) is superior to μ_{H2O} (1.88Debye) [65]. The found low energy gap and the high value of dipole moment cause electrons exchange from the molecule to the surface. This takes place during the adsorption process on the carbon steel area.

The molecular stability and molecular reactivity are related to the measured absolute hardness and softness. A large energy gap characterizes a hard molecule and a small one distinguishes a soft molecule. Because it is difficult to the hard molecules to give electrons to an acceptor, their reactivity is less than the soft ones. Adsorption could occur at the part of the molecule where σ has the highest value [33]. It is demonstrated that the inhibition efficiency will be high because of the low value of the global hardness which is equal to 2.34eV and the high value of the global softness 0.43 (Table 5). This result agrees with the literature [33, 34, 36]. Thus, the low value of the energy gap between the frontier molecular orbitals of the inhibitor confirms the reactivity of the inhibitor molecule with metal atoms.

Generally, the value of ω affects the inhibition efficiency. The latter increases with the decrease of the ω value. The electrophilicity index (ω) of MMBI which is equal to 2.05 confirms the high value of the inhibition rate [91].

According to Lukovits [92], the chemisorption and inhibition effectiveness increases with the elevating in the electron transfer ability to the metal surface. This shows that as the strength of the iron-inhibitor bond increases (as a result of the increase of ΔN), the degree of corrosion inhibition due to chemisorptions is increased. As previously cited in the literature, the chemisorption of inhibitor molecules provides higher corrosion inhibition when compared to physic-sorption process. According to the experimental data, the corrosion inhibition efficiency of MMBI is high. This is manifested by the high number of electrons transferred (ΔN) which has been found to be equal to 0.83 confirming the good inhibition efficiency and good chemical adsorption of this benzimidazole derivative. From Table 5, the low electrophilicity ω = 2.05 and the high fraction of electrons transferred value ΔN=0.83 agree with the good and high inhibition efficiency of the studied inhibitor. Table 5 shows that ΔN is positive and less than 3.6 [93, 94], confirming that the inhibitor can donate electrons to iron to form coordinate bonds and results consequently an adsorption inhibitive layers against corrosion.

The electronegativity value of the inhibitor molecule was found to be 3.1 which is inferior than that of iron, suggesting an electron transfer from the HOMO of the inhibitor towards the empty 3d orbital of Fe. This electron exchange is more significant than that from the occupied 4s orbital of Fe to LUMO of the inhibitor.

The lower value of χ may be due to the elevated electronegativity of the nitrogen atom over the carbone one as well as the existence of a more electronegative oxygen atom in the substituted methoxy phenyl group. So, the electron flow from benzimidazole substituted compound is strongly more favorable to higher inhibition efficiency [5].

Because the Molecular Electrostatic Potential (MEP) is related to electronic density and in ordre to determine the sites of electrophilic and nucleophilic reactions, the MEP was used as a useful descriptor [95]. We used the optimized geometry of the MMBI to determine its reactive sites for electrophilic and nucleophilic attack. Fig.10 shows the mapped electron density surface with the MEP of MMBI. The red and yellow colors in MEP map indicate the electrophilic active region. The nucleophilic ones are colored in light blue and blue. In MEP contours, the yellow and red color lines present the positively charged and negatively charged regions, respectively.

The last figure shows clearly that the more electron rich regions are mainly localized around the heteroatoms and the conjugated double bonds. The electrophilic active sites are localized in the center of molecule around the oxygen (O37 and O42) and nitrogen atoms (N11 and N12). According this, oxygen and nitrogen atoms give nucleophilic reactions in the corrosion inhibiting process [91].

The studied and promoted MMBI can give chelate species on the mild steel surface by exchanging electrons between benzimidazole groups and iron atom (d-orbital) to form coordinate covalent bond through the chemical adsorption process. In this fact, the XC52 steel acting as an electrophile can attract the negatively charged sites of the MMBI molecule. The nucleophilic centers of these molecules are heteroatoms with free electron pairs, functional electronegative groups and p-electrons in conjugated double bonds, which are available to form chemical bonds [96].

Fig.10 indicates that adsorption of the studied inhibitor is mostly governed by the electron transfer from the HOMO of the inhibitor to the vacant metal d orbital. It is clearly seen that HOMO energy level of the molecule is mostly distributed over the planar Benzimidazole group and the methoxy phenyl substituent [97].

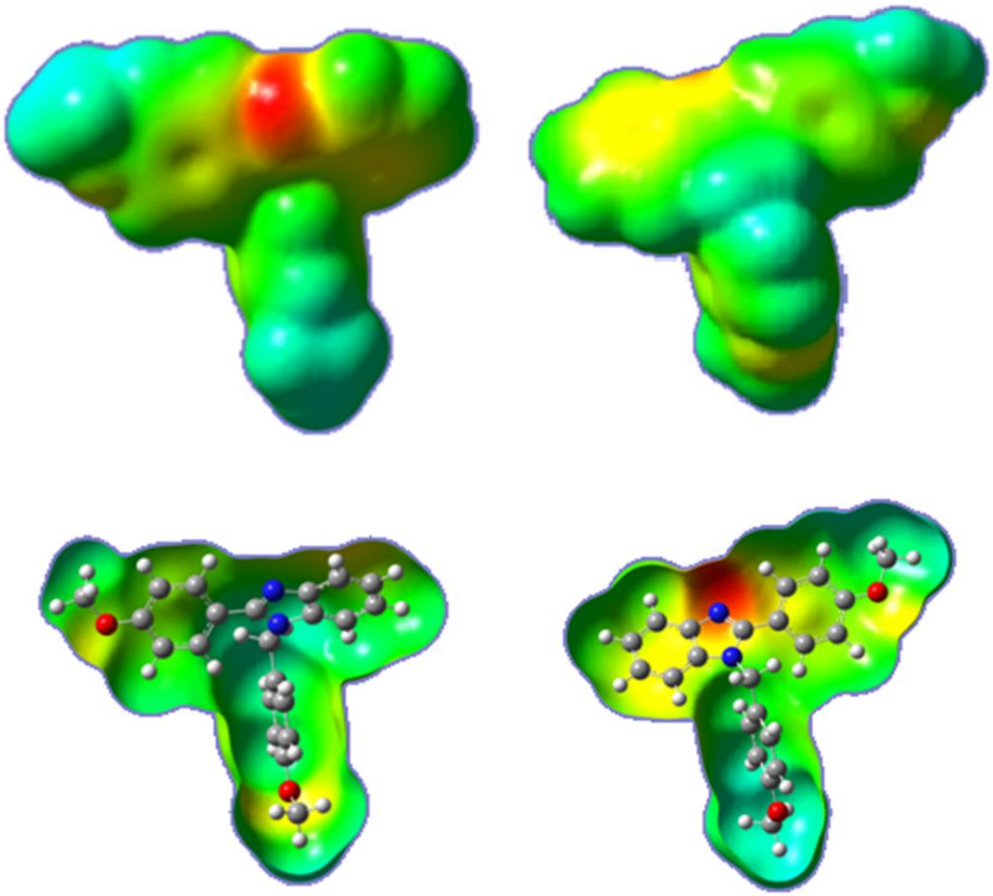

(a) (b)

Figure 10. MEP map and counter plot of the studied inhibitor. (a) Front view and (b) Rear view.

The Mulliken charge related to the vibrational properties of the molecule evaluates the way how the atomic displacement affects the electronic structure charge. The more negatively charged heteroatom can be adsorbed on the metal surface, through a donor-acceptor type reaction [98, 99].

The Mulliken charges of the atoms, determined for the studied inhibitor (Table 6), indicate that the more negative atoms are found to be N11, N12, O37 and O42 which are active adsorptive centers. This agrees perfectly with the literature results [100].

Natural bonding orbitals (NBO) analysis is an efficient method for investigating intra- and inter-molecular bonding and interactions among bonds. It is also provides a convenient basis for studding charge transfer or conjugative interaction in molecular systems [101]. The interactions between the filled orbitals of one subsystem and vacant orbitals of another system were studied. The calculated NBO values were given in Table 6. It is noted that the nitrogen, the oxygen and some

carbon atoms of benzimidazole, benzyl and methoxyphenyl rings of the inhibitor have negative charges. Thus, they are favored sites for adsorption on to the XC52 steel area.

According to Table 5 no significant differences are observed in the calculated chemical quantum parameters in aqueous phases (water) and gas phase except for the dipole moment (μ). This parameter considerably increased during the passage from the gas phase to the aqueous phase. The polarization of the molecule induced by the molecule-solvent interaction explains this increase.

The results show that our studied molecule has a low value of gap energy. This confirms the elevate reactivity of MMBI as well the high inhibition efficiency. This is in good agreement with experimental investigations.

Table 6. Calculated Mulliken atomic charges of the MMBI.

	Gas phase		Aqueous phase	
Atom	Mulliken charges	NBO charges	Mulliken charges	NBO charges
C_1	-0,098	-0.257	-0,115	-0.264
C_2	-0,126	-0.231	-0,149	-0.246
C_3	0,225	0.117	0,216	0.109
C_4	0,301	0.132	0,302	0.131
C_5	-0,110	-0.274	-0,121	-0.274
C_6	-0,109	-0.242	-0,127	-0.250
H_7	0,078	0.239	0,096	0.247
H_8	0,090	0.247	0,098	0.250
H_9	0,090	0.244	0,111	0.254
H_{10}	0,079	0.239	0,099	0.248
N_{11}	-0,589	-0.401	-0,582	-0.392
N_{12}	-0,561	-0.492	-0,600	-0.528
C_{13}	0,415	0,420	0,420	0.428
C_{14}	-0,115	-0,258	-0,117	-0.271
H_{15}	0,141	0.265	0,152	0.271
H_{16}	0,128	0.253	0,147	0.264
C_{17}	-0,115	-0.266	-0,133	-0.276
C_{18}	-0,120	-0.222	-0,129	-0.223
C_{19}	0,089	-0.087	0,084	-0.089
C_{20}	-0,122	-0.223	-0,138	-0.231
C_{21}	-0,139	-0.315	-0,152	-0.319
C_{22}	0,352	0.319	0,347	0.315
H_{23}	0,097	0.252	0,105	0.255
H_{24}	0,082	0.238	0,104	0.250
H_{25}	0,105	0.253	0,107	0.253
H_{26}	0,091	0.254	0,112	0.255
C_{27}	0,063	-0.130	0,054	-0.139
C_{28}	-0,104	-0.174	-0,109	-0.192
C_{29}	-0,142	-0.322	-0,138	-0.282
C_{30}	0,357	0.329	0,356	0.331
C_{31}	-0,130	-0.276	-0,156	-0.321
C_{32}	-0,123	-0.215	-0,131	-0.205
H_{33}	0,116	0.261	0,110	0.259
H_{34}	0,090	0.244	0,109	0.257

H_{35}	0,098	0.252	0,117	0.258
H_{36}	0,101	0.247	0,111	0.252
O_{37}	-0,516	-0.517	-0,529	-0.524
C_{38}	-0,081	-0.329	-0,095	-0.335
H_{39}	0,114	0.207	0,130	0.216
H_{40}	0,126	0.233	0,137	0.239
H_{41}	0,116	0.208	0,130	0.216
O_{42}	-0,519	-0.520	-0,534	-0.530
C_{43}	-0,080	-0.329	-0,092	-0.334
H_{44}	0,113	0.207	0,126	0.214
H_{45}	0,114	0.207	0,126	0.214
H_{46}	0,126	0.233	0,135	0.238

4. CONCLUSION

An heterocyclic and eco-friendly inhibitor namely: (4-methoxybenzyl)-2-(4-methoxyphenyl)-1H-benzimidazole was synthesized with no use of the catalyst substance. MMBI showed important inhibitive properties against the corrosion of a pipeline steel sample grade XC52 in a 1M HCl solution. It was found that the inhibition effectiveness increases with increasing the inhibitor's concentration.

The results of potentiodynamic polarization measurements demonstrated that benzimidazole derivative acts as a mixed type inhibitor with a predominant cathodic effectiveness. MMBI prevents XC52 steel corrosion. This protection occurs from the spontaneous adsorption of inhibitor on mild steel surface. The mechanism obeys Langmuir isotherm. The thermodynamic adsorption characteristics such as $\Delta G°_{ads}$, E_a and K_{ads} confirmed that the inhibitor is effectively adsorbed by a chemisorption process.

The quantum chemical study revealed that the theoretical results agree with the experimental ones. The low value of the gap energy between E_{HOMO} and E_{LUMO} favors the adsorption of MMBI on the steel surface and enhances the protecting power of inhibitor.

As a result of MEP, it can be noted from the distribution of the electron density that oxygen and nitrogen atoms are the appropriate heteroatom for the interaction in the inhibition of the corrosion process. It was revealed that the sites N11, N12, O37 and O42 are most favorable for electrophilic attack and consequently, they present more opportunity to form bonds with the steel surface. The NBO results are in perfect accordance with those provided by MEP analysis.

ACKNOWLEDGEMENTS
The authors gratefully acknowledge the financial support from the Algerian Ministry of Higher Education and Scientific Research. The authors would like to thank Professor Bernard Spiess from Laboratoire d'Innovation Thérapeutique - UMR 7200 Faculté de Pharmacie - 74, route du Rhin, BP 60024 67401 Illkirch Strasbourg France, and Professors Mehmet Erbil and Tunç Tüken from Faculty of Science and Letters Chemistry Department Çukurova University Turkey for helpful.

References

1. Ron Jarvis CEng MIChemE, Swiss Re, London Andy Goddard CEng MIChemE, Talbot Underwriting, London LMA OG&P Loss Analysis – Version 1.0 (September 2016).

2. M. Finšgar and J. Jackson, *Corros. Sci*., 86 (2014) 17.
3. X. Wang, Y. Wan, Y. Zeng and Y. Gu, *Int. J. Electrochem. Sci*., 7 (2012) 2403.
4. A. Popova, M. Christov and T. Deligeorgiev, *Corrosion*, 59 (9) (2003) 756.
5. A, Dutta, S.S. Panja, M.M. Nandi and D. Sukul, *J. Chem. Sci.,* 127 (5) (2015) 921.
6. O. Olivares-Xometl, N.V. Likhanova, B. Gómez, J. Navarrete, M.E. Llanos-Serrano, E. Arce and J.M. Hallen, *Appl. Surf. Sci.,* 252 (2006) 2894.
7. O. Olivares-Xometl, N.V. Likhanova, M.A. Domínguez-Aguilar, E. Arce, H. Dorante and P. Arellanes-Lozada, *Mater. Chem. Phys*., 110 (2008) 344.
8. U. Ergun, D. Yüzer and K.C. Emregül, *Mater. Chem. Phys*., 109 (2008) 492.
9. S.M. Salih, M.A. Fadhil, *J. Appl. Chem.,* 89 (2016) 505.
10. K.R. Ansari, M.A. Quraishi, and A. Singh, *Measurement*, 76 (2015) 136.
11. J. Cruz, R. Martínez-Palou, J. Genesca and E. García-Ochoa, *J. Electroanal. Chem.,* 566 (2004) 111.
12. O. Olivares-Xometl, N.V. Likhanova, R. Martínez-Palou and M.A. Dominguez-Aguilar, *Mater. Corros.,* 60 (2009) 14.
13. N.V. Likhanova, R. Martínez-Palou, M.A. Veloz, D.J. Matías, V.E. Reyes-Cruz and O. Olivares-Xometl, *J. Heterocycl. Chem.,* 44 (2007) 145.
14. T.K. Chaitra, K.N.S. Mohana and H.C. Tandon, *J. Mol. Liq.,* 211 (2015) 1026.
15. M. Bouanis, M. Tourabi, A. Nyassi, A. Zarrouk, C. Jama and F. Bentiss, *Appl. Surf. Sci.,* 389 (2016) 952.
16. D.E. Tallman, G. Spinks, A. Dominis and G.G. Wallace, *J. Solid State Electrochem.,* 6 (2002) 73.
17. M. Finšgar and J. Jackson, *Corros. Sci*., 86 (2014) 17.
18. M.A. Quraishi, H.K. Sharma, Material Chemistry and Physics. 78 (2003) 18-21.
19. P. Morales-Gil, G. Negrón-Silva, M. Romero-Romo, C. Ángeles-Chávez and M. Palomar-Pardavé, *Electrochim*. *Acta*., 49 (2004) 4733.
20. F. Bentiss, M. Lagrenee, M. Traisnel and J.C. Hornez, *Corros. Sci*., 41 (4) (1999) 789.
21. Y. Abboud, A. Abourriche, T. Saffaj, M. Berrada, M. Charrouf, A. Bennamara, A. Cherqaoui and D. Takky, *Appl. Surf. Sci.,* 252 (2006) 8178.
22. X. Wang, H.Yang and F. Wang, *Corros. Sci*., 53 (2011) 113.
23. M. Benabdellah, A. Tounsi, K.F. Khaled and B. Hammouti, *Arab. J. Chem*., 4 (2011) 17.
24. Y. Abboud, B. Hammouti, A. Abourriche, B. Ihssane, A. Bennamara, M. Charrouf and S.S Al-Deyab, *Int. J. Electrochem. Sci*., 7 (2012) 2543.
25. N.S. Patel, S. Jauhari and G.N. Mehta, *Acta Chim. Slov.,* 57 (2010) 297.
26. R.R. Moreira, T.F. Soares and J. Ribeiro, *Adv. Chem. Engineer. Sci.,* 4 (2014) 503.
27. A. Popova, M. Christov and A. Vasilev, *Corros. Sci*., 94 (2015) 70.
28. N. Esmaeili, J. Neshati and I. Yavari, *Res. Chem. Intermed.,*42 (2016) 5339.
29. A. Popova, E. Sokolova, S. Raicheva and M. Christov, *Corros. Sci*., 45 (2003) 33.
30. A. Popova, M. Christov, S. Raicheva and E. Sokolova, *Corros. Sci*., 46 (2004) 1333.
31. A. Popova, M. Christov and A. Zwetanova, *Corros. Sci*., 49 (2007) 2131.
32. J. Aljourani, K. Raeissi and M.A. Golozar, *Corros. Sci*., 51 (2009)1836.
33. A. Aouniti, H. Elmsellem, S. Tighadouini, M. El azzouzi, S. Radia, A. Chetouani, B. Hammouti and A. Zarrouk, *J Taibah Univ Sci.,* 10 (2016) 774.
34. M. Yadav, S. Kumar, T. Purkait , L.O. Olasunkanmi, I. Bahadur and E.E. Ebenso, *J. Mol. Liq.,* 213 (2016) 122.
35. R.S. irami, M. Amirnasr, K. Raeissi, M.M. Momeni and S. Meghdadi, *J. Iran. Chem. Soc*., 12 (2015) 2185.
36. I.B. Obot, D.D. Macdonald and Z.M. Gasem, *Corros. Sci*., 99 (2015) 1.
37. H.R. Obayes, G.H. Alwan, A.H.MJ. Alobaidy, A.A. Al-Amiery, A.A.H. Kadhum and A.B. Mohamad, *Chem. Cent. J.,* 21 (2014) 1.
38. O.R. Shehab and A.M. Mansour, *J. Mol. Struct.,* 1047 (2013) 121.

39. A.M. Mansour, *Inorg. Chim. Acta.,* 408 (2013) 186.
40. M. Karnan, V. Balachandran , M. Murugan and M.K. Murali, *Spectrochim Acta A Mol Biomol Spectrosc*., 130 (2014) 143.
41. E. Garcia-Ochoa, S.J. Guzmán-Jiménez, J. Guadalupe Hernández, T. Pandiyan, J.M. VásquezPérez and J. Cruz-Borbolla, *J. Mol. Struct.,* 1119 (2016) 314.
42. M. Abreu-Quijano, M. Palomar-Pardavé, A. Cuán, M. Romero-Romo, G. Negrón-Silva,
43. R. Álvarez-Bustamante, A. Ramírez-López and H. Herrera-Hernández, *Int. J. Electrochem. Sci*., 6 (2011) 3729.
44. Pedro de Lima-Neto , A.P. de Araújo, W.S. Araújo and A.N. Correia, *Prog. Org. Coat.,* 62 (3) (2008) 344.
45. S.A. Ali, H.A. Al-Muallem, M.T. Saeed and S.U. Rahman, *Corros. Sci*., 50 (2008) 664.
46. D. Wahyuningrum, S. Achmad, Y.M. Syah, Buchari, B. Bundjali and B. Ariwahjoedi, *Int. J. Electrochem. Sci*., .3 (2008) 154.
47. K.F. Khaled, *Electrochim. Acta*., 53 (2008) 3484.
48. X. Wang, *Int. J. Electrochem. Sci*., 7 (2012) 11149.
49. V.Z. Mota, G.S.G. de Carvalho, A.D. da Silva, L.A. S.Costa, P.de Almeida Machado, E.S. Coimbra, C.V. Ferreira, S.M. Shishido and A. Cuin, *Biometals,* 27 (2014) 183.
50. M. Banerjee, A. Chatterjee, V. Kumar, Z.T. Bhutia, D.G. Khandare, M.S. Majik and B.G. Roy *Electronic Supplementary Material (ESI) for RSC Advances*, (2014) 1.
51. S.H. Nile, B. Kumar and S.W. Park, *Arab. J. Chem*., 8 (5) (2015) 685.
52. S.D. Sharma and D. Konwar, *Synth. Commun.,* 39 (2009) 980.
53. B. Kumar, K. Smita, B. Kumar and L. Cumbal, *J. Chem. Sci.,* 126 (2014) 1831.
54. A.D. Becke, *J. Chem. Phys.,* 98 (1993) 5648.
55. C. Lee, W. Yang and R.G. Parr, *Phys. Rev. B.*, 37 (1988) 785.
56. M. Frisch, G. Trucks, H. Schlegel, G. Scuseria, M. Robb, J. Cheeseman, G. Scalmani, V. Barone, B. Mennucci and G. Petersson, Gaussian 09, Revision A. 1,Gaussian Inc., Wallingford, CT. (2009)
57. R. Dennington, T. Keith and J. Millam, GaussView, Shawnee Mission, KS: Semichem, Incorporated Company Officers (2009).
58. R.G. Parr and R.G. Pearson, J. *Am. Chem. Soc.,* 105 (12) (1983) 7512.
59. A.Y. Musa, A.A.H. Kadhum, A.B. Mohamed and M.S. Takriff, *Mater. Chem. Phys.,* 129 (2011) 660.
60. F. Zhang, Y.M. Tang, Z. Cao, W. Jing, Z. Wu and Y. Chen, *Corros. Sci*., 61 (2012) 1.
61. M. Behpour, *J. Mater. Sc*., 44 (2009) 2444.
62. M. Bouanisa, M. Tourabia, A. Nyassia, A. Zarroukb, C. Jamac and F. Bentissal, *Appl. Surf. Sci.,* 389 (2016) 952.
63. I. Ahamad, R. Prasad and M.A. Quraishi, *Corros. Sci*., 52 (2010) 1472.
64. J.O.M. Bockris and S. Srinivasan, *Electrochim. Acta.*, 9 (1964) 31.
65. M. Behpour, S.M. Ghoreishi, N. Soltani and M. Salavati-Niasari, *Corros. Sci*., 51 (2009) 1073.
66. H.M. Abd El-Lateef, A.M. Abu-Dief and M.A.A. Mohamed, *J. Mol. Struct.,* 1130 (2017) 522.
67. S.M. Tawfik and M.F. Zaki, *Res. Chem. Intermed.,* 41 (11) (2015) 8747.
68. A. Doner, R. Solmaz, M. Ozcan and G. Kardas, *Corros. Sci*., 53(2011) 2902.
69. R. Solmaz, *Corros. Sci*., 79 (2014) 169.
70. M.A. Hegazy, M. Abdallah, M.K. Awad and M. Rezk, *Corros. Sci*., 81 (2014) 54.
71. B. Xu, W. Yang, Y. Liu, X. Yin, W. Gong and Y. Chen, *Corros. Sci*., 78 (2014) 260.
72. F. Mansfeld, M.W. Kending and S. Tsai, *Corrosion,* (a) 37 (5) (1981) 301-307, (b) 38 (1981) 570.
73. T. Tsuru, S. Haruyama and B. Gijutsu, J. *Japan Soc. Corros. Eng.,* 27 (1978) 573.
74. M. Cafferty and E. Hackerman, *J. Electrochem. Soc.,* 119 (8) (1972) 999.
75. G. Avci, *Colloids and Surfaces A: Physicochem. Eng. Aspects.,* 317 (2008) 730.
76. M. Elayyachy, A. El Idrissi and B. Hammouti, *Corros. Sci*., 48 (2006) 2470.

77. F.M. Donahue and K. Nobe, *J. Electrochem. Soc.,*112 (9) (1965) 886.
78. Z. Salarvand, M. Amirnasr, M. Talebian, K. Raeissi and S. Meghdadi, *Corros. Sci*., 114 (2017) 133.
79. R. Mohan, K.K. Anupama and A. Joseph, *J. Bio. Tribo. Corros.,* 3 (2) (2017) 1.
80. E. Bayol, T. Gurtenb, A.A. Gurtena and M. Erbil, *Mater. Chem. Phys.,* 112 (2008) 624.
81. O. RADOVICI, Proc. 7th European, symposium on corrosion inhibitors, Annali dell' Università di Ferrara, Italy. (1990) 330.
82. S. Martinez and I. Stern, *Appl. Surf. Sci.,*199 (2002) 83.
83. D.M. Gurudatt and K.N. Mohana, *Journal of Applicable Chemistry*, 2 (2013) 1296.
84. V.R. Saliyan and A.V. Asudeva, *Bull. Mater.* Sci., 31 (4) (2007) 699.
85. R.S. Erami, M. Amirnasr, K. Raeissi, M.M. Momeni and S. Meghdadi, *J. Iran. Chem. Soc.,* 12 (2015) 2185.
86. L.M. Rodrıguez-Valdez, W. Villamisar, M. Casales, J.G. Gonzalez-Rodriguez, A. Martınez-Villafane, L. Martinez and D. Glossman-Mitnik, *Corros. Sci*., 48 (2006) 4053.
87. V. Sastri and J. Perumareddi, *Corrosion,* 53 (1997) 617.
88. M.M. Kabanda, L.C. Murulana, M. Ozcan, F. Karadag, I. Dehri, I.B. Obot and E.E. Ebenso, *Int. J. Electrochem. Sci., 7 (2012) 5035.*
89. S. Martinez and I. Stagljar, *J. Mol. Struct.,* 640 (2003) 167.
90. M.A. Amin, K.F. Khaled and S.A. Fadl-Allah, *Corros. Sci*., 52 (2010) 140.
90. G. Gece and S. Bilgic, *Corros. Sci*., 51 (2009) 1876.
91. F. Mohsenifar, H. Jafari and K. Sayin, *J. Bio. Tribo. Corros.,* 2(1)(2016) 1.
92. I. Lukovits, E. Klaman and F. Zucchi, *Corrosion,* 57 (2001) 3.
93. N. Kovačević and A. Kokalj, *Corros. Sci*., 53 (2011) 909.
94. B. Xu, W.Gong, K. Zhang, W. Yang, Y. Liu, X. Yin, H. Shi and Y. Chen, *J. Taiwan. Inst. Chem. Eng.*, 51 (2015) 193.
95. N. Okulik and A.H. Jubert, *Internet Electron. J. Mol. Des.,* 4 (2005) 17.
96. H. Tian, W. Li, K. Cao and B. Hou, *Corros. Sci*., 73 (2013) 281.
97. Y. Tang, *Corros. Sci*., 74 (2013) 271.
98. N.O. Obi-Egbedi, K.E. Essien, I.B. Obot and E.E. Ebenso, *Int. J. Electrochem. Sci.,* 6 (2011) 913.
99. M. Ozcan, I. Dehri and M. Erbil, *Appl. Surf. Sci.,* 236 (2004) 155.
100. J.M. Roque, T. Pandiyan, J. Cruz and E. Garcı´a-Ochoa, *Corros. Sci*., 50 (2008) 614.
101. M. Snehalatha, C. Ravikumar, I. H. Joe, N. Sekar and V.S. Jayakumar, *Spectrochim. Acta A Mol. Biomol. Spectrosc.*, 72 (2009) 654.